

EVS25

Shenzhen, China, Nov 5-9, 2010

Electric Vehicles – Personal transportation for the future

Grant A. Covic¹, John T. Boys¹, Mickel Budhia¹, Chang-Yu Huang¹

¹ Department of Electrical and Computer Engineering, The University of Auckland, Private Bag 92019, Auckland

1142, New Zealand

E-mail: ga.covic@auckland.ac.nz

Abstract

Plug-in EVs are being heralded as a step towards acceptance of pure EV's. However concerns remain regarding uptake by consumers, in terms of range anxiety and economic operation. These concerns are mitigated if energy can be transferred to the vehicle while it is moving, but there are implications in terms of the highway infrastructure required without restricting a vehicle's freedom to move while providing power over air-gaps in excess of 200mm. Such flexibility brings with it problems that are not normally inherent in stationary systems where electronic alignment may be employed to control magnetic coupling. The system must cope with variances as seen by both the power supply and the EV, while ensuring that the power receiver is compatible with both stationary and roadway systems. This paper discusses recent developments in wireless charging infrastructure for EV's and describes systems that may be suitable in future. As vehicles operate on the Grid they will constitute a substantial load that must be managed. A solution is presented here at little infrastructural cost such that the Grid, 'on load' has better power quality than 'off-load'.

Keywords: Inductive power transfer, Electric vehicle charging, Dynamic demand control

1 Introduction

For some time Electric Vehicles have been proposed for transportation in the future but they have not gained overall acceptance, and the technology has remained as one for enthusiasts. Reasons for this are many but a prime one is likely that the technology has always been expensive in compared with conventional vehicles, and there are always other choices such as fuel cells, hydrogen in general, bio-fuels, flywheels, hybrids, and others. Against this an EV solution has had to justify battery technologies

that are expensive and short-lived, and charging systems that are costly new technology. Indeed compared with a conventional vehicle an EV is twice as expensive and a hybrid is three times the cost – a Toyota corolla at \$15k compares with a hybrid containing essentially a conventional car, a battery at much the same cost, and all of an electric car at much the same cost again.

Hydrogen power is attractive as it can be refueled at refueling sites similar to conventional gas-stations, and hydrogen is an excellent fuel. Here the major weight in the fuel is oxygen that does not have to be carried at all. Electric vehicles

have to carry all of the energy to drive them and the cost and weight of this stored energy is very high. Indeed [1] shows that no EV of any type can compete with a conventional vehicle for cost of ownership without government subsidies, except a hypothetical EV where electrical energy is picked up from the roadway as the car travels: this technology without subsidy, and including an overhead charge of US\$1000/vehicle, is in fact lower cost than a conventional vehicle - but the technology to support it is still not there.

Today in the USA there is bi-partisan support to develop an infrastructure for the electrification of their roadway system in the interests of National Security. Arguably the country cannot spend trillions of dollars per year importing gasoline from all over the world when such importation is compromising its economy and the situation will only get worse. Even at this very early stage it is clear that the cost will be high - perhaps US\$200B but this cost, while high, is a small fraction of the cost of gasoline in the future if nothing is done.

An electrified transportation fleet has advantages: it can run on almost any fuel – wind, solar, nuclear, woody bio-mass, tidal, wave – and it is easy to keep it carbon free or at least carbon neutral. Dynamic demand control (DDC) of the grid means that energy can be fed into the grid system when it is available and the electric vehicle fleet will vary its uptake dynamically to maintain the grid and improve the quality of power to all other users. There is no other power application of such magnitude that can control the grid and improve the power quality while allowing renewable energies to feed directly into the network. Further, bidirectional chargers allow the batteries of stationary EV's to act as an energy store for the grid and supply peak power as required. With a large number of EV's the energy storage can be very high but the economics of this technique must balance the cost of the scheme against the cost of cycling the batteries.

Hardware to build electrified transportation systems have been presented in papers over the past 20 years. Early US patents 4331225, 4836344 and 6879889 amongst others have proposals to allow vehicles to pick-up power inductively while driving (now called Dynamic Inductive Powered Transportation (DIPT)), but to date none has been implemented up to now the technology lacked utility, and was not cost competitive with gasoline. These drawbacks are

now invalid and significant work in the last decade has realized systems whereby moving vehicles can be powered over suitable air-gaps at levels required by modern EV's with both single and multiphase systems [2]. Such systems comprise a sequence of coils set in a continuous strip along the road. A vehicle follows this strip and picks off power magnetically as shown in Fig. 1. In this system, current I_1 is generated at VLF frequency (typically 10-80 kHz) in a loop of wire called a track and power is magnetically coupled to the pick-up receiver on the vehicle. The power transfer is described by (1), where the uncompensated power (P_{su}) is given by the product of the open circuit voltage (V_{oc}) and the short circuit current (I_{sc}) of the receiver coil (L_2). To boost power the secondary is tuned for operation at the track frequency (ω) and the quality factor Q represents this boost in the receiver on the EV (typically $3 < Q < 6$ to allow for component tolerances). M is the mutual inductance between the track and the pick-up receiver.

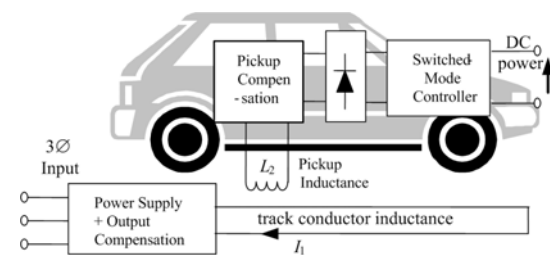


Figure 1: A typical IPT system

Increasing the power and separation between the track and the receiver on the vehicle is desirable for air-gaps of 100-300mm. A well designed system is in general tolerant to misalignment and variable air-gap lengths but with roadway applications such variations are likely to be extreme and some mechanisms may be needed to help with automatic alignment.

$$P_{out} = P_{su}Q = V_{oc}I_{sc} = \omega I_1^2 \frac{M^2}{L_2} Q \quad (1)$$

This paper presents both simulated and experimental measurements on technology for roadway powered electric vehicles, including measurements for a wind-powered system operating with an inductive power charging system at laboratory scale.

2 System Overview

2.1 A Possible IPT Roadway System

Electric vehicles reduce dependence on fossil fuels and emission of greenhouse gasses and pollutants. Consequently, EV uptake has been increasing however market penetration has been low because EVs are less cost effective than conventional vehicles. The present EV market is dominated by hybrid vehicles that derive their energy from an IC engine, but, plug-in EVs (PHEV) have recently been introduced enabling grid energy to mitigate gasoline consumption. In order for EVs to gain widespread adoption, major improvements are required in battery life and cost, and grid connection. The latter allows opportunistic charging after each trip rather than a single long daily charge. Battery wear is significantly reduced by minimizing the depth of discharge, and the EV has a lower cost since a smaller battery is required [1],[3,4]. The preferred solution, making EVs more cost effective than gasoline vehicles, as discussed in [1], is to power and recharge the EV via the road. The infrastructure for such a dynamic charging system could be relatively small since while interstate highways make up only 1% of roadway miles, they carry 22% of all vehicle miles travelled. An EV that has 50% of its driven miles connected to a dynamic charging system would be as cost effective as a conventional vehicle [1, 3].

The purpose of this research is to investigate a practical Inductive Power Transfer (IPT) system powering and recharging EVs moving along a roadway, completely minimizing onboard energy storage and hence vehicle weight and cost. Fig. 2 shows a possible configuration of such a highway system. Power supply cabinets can be placed alongside the highway at suitable spacing (say 20-200m). Within each cabinet there exists one or more suitable resonant power supplies capably of energizing one or more pads placed along the centre of a highway lane. Only pads that are underneath a vehicle that is able to receive power from the roadway should be energized. This ensures that other vehicles can travel along the roadway without acting as an undesirable load, and that conventional vehicles are not heated by magnetic fields. To transfer sufficient power one or more pads sitting underneath a moving vehicle will need to be energized, requiring suitable detection means for the position of the vehicle, and means to switch roadway pads on and off sequentially, while supplying each with an appropriate current.

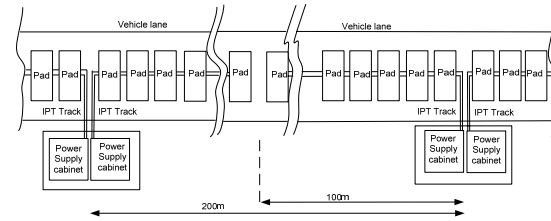


Figure 2: A Possible IPT Powered Highway

A power input of 10-30kW to an EV is sufficient for motive power and charging while driving in various situations such as urban, highway and mountainous terrains [5, 6]. The energy collected by the EV depends on the length of powered road, and the vehicle speed. Additionally, the placement of powered sections on steep sections of roadway is desirable to limit the discharge rate of the vehicle battery and to prolong its life. For the DIPT system proposed here, each pad should be capable of delivering at least 10kW to a vehicle and these pads should be no bigger than one or two meters square. Consequently larger vehicles may well couple to two or more pads to receive higher power transfer rates as required. Furthermore, while IPT systems have been discussed for some time, large scale systems have to date appeared impractical due to the challenge of coupling such power with large horizontal tolerances ($\sim\pm 350\text{-}\pm 700\text{mm}$) while meeting ground clearances of 100-300mm required by various EVs. For North American highways there is a further demand, in that any pad on the road must be covered by 50-75mm of asphalt. Naturally the focus over the last decade has therefore been on lumped systems for EV's at modest power levels (2-3kW) for home based charging. The magnetic designs of such systems are naturally focused on power transfer at a defined location, and often assume some guided assistance for parking. The challenge therefore is how to ensure these magnetic designs are future proofed and suitable for both stationary and moving applications. The following section discusses recent magnetic developments for EV charging and focuses particularly on those that could be scaled to the levels now required.

With today's Power Systems there is an increasing emphasis in 'green' power achieved using renewable sources with little or no carbon footprint. Such sources include wind, wave, and tidal power all characterized by being fluctuate to such extent that the power from them cannot be guaranteed even for only a few minutes into the future. These sources are important as they are carbon free but their use means that the grid

frequency cannot be held as precisely as has now come to be expected. Electric vehicles will therefore at various times be driven by green power when parked charging, or when moving powered by IPT where they must maintain their roadway position at the required speed. There are two fail-safe conditions that the home or roadway based power supply must meet: a situation where grid power is temporarily not available, and a situation where the power required exceeds the rating of the power supply. Variations are many and include the condition where a large surge of power is available and vehicles may use it to charge their batteries, even though it is only a temporary surge.

There are current proposals for solving the power system problem. It has been suggested that all PHEV chargers could be fully reversible so that when the vehicle is parked up and charging overnight the electricity company can reverse the charging process and drain energy from the batteries of all the vehicles on charge to meet a temporary power demand. Such a power reversal would need significant communications over a whole country/region and would have to be very fast acting to avoid spectacular collapses as the power system becomes overloaded. As more generators drop out the frequency decreases more rapidly and the condition worsens. If all the reversible battery chargers could be reversed the process might be saved but such power reversal would have to occur very quickly – probably in less than 5 seconds - in the collapsing power system to save it.

With DDC implemented within the home based charging and roadway network, this problem is mitigated. When the power system has a lot of wind power added to it at times of wind surges the mains frequency will increase slightly and with DDC implemented this will signal the battery charging to increase where possible. Conversely when the wind dies the charging can be reduced, and even with dynamic charging the battery energy will easily provide a 'ride-through' period. In concept, if upwards of 20kW is being transferred to each vehicle along a highway and this is split evenly (10kW for motive power and 10kW for charging), up to 10kW/vehicle can be instantly shed (that required for charging) without effecting the battery on-board battery capacity. A further 10kW/vehicle may be available providing the on-board battery is sufficiently charged to be able to be discharged for the period required.

Thus an EV system with power supplies and batteries operating under DDC will improve the quality of supply with wind generation as it will help to stabilize the frequency. Such a system is shown conceptually in Fig. 3 where conventional generators supply conventional consumer loads, but energy based loads such as EV's are used to accept the variable energy supplied by fluctuating sources such as wind. This aspect is discussed in further detail in section Four.

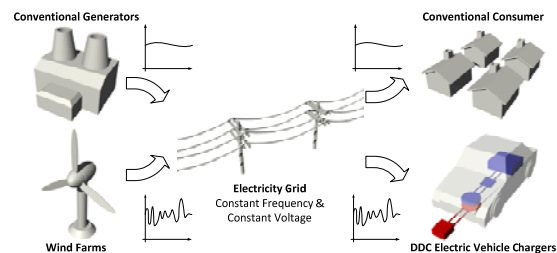


Figure 3: DIPT can be improved with DDC to improve the power network and utilize increased green energy.

3 Charging Pad Developments for EVs

3.1 Single Phase Charging Pads

The most common inductive charging system proposed to couple flux between a primary transmitter and secondary receiver has a circular magnetic structure. Both the ground and receiver pad are nominally identical. Each has six main components shown in the exploded view of Fig. 4. The aluminum ring and backing plate shield the chassis of the EV and surrounding area from stray magnetic fields [7]. Alternative power couplers are; pot cores [8], U-shaped cores [9], ferrite discs or plates [10-11] or E-cores [12]. All of these are comparatively fragile and expensive due to the geometry of the large pieces of ferrite required to achieve the desired power transfer flux path.

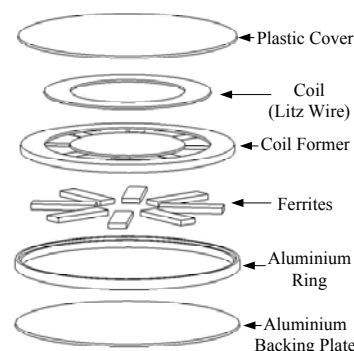


Figure 4: Exploded view of a power pad

Arrays of coils with ferrite backing allow power transfer over large areas with low power systems in [13] however this technique is not cost effective for higher power EV charging systems. As shown in [14], each row or column of coils needs to be switched to prevent field cancellation in the centre of the multilayer array to increase the power transfer - this is impractical with high power systems. Coreless coils as shown in [15] are generally not suitable for high power applications with conductive or ferrous materials close to the system. Field shaping with ferrite constrains flux to desired paths improving coupling and preventing excessive energy loss in surrounding materials. As shown in (1), the mutual inductance between couplers and the primary current have the greatest influence on power transferred. To compensate for lower coupling and maintain good efficiency, coreless systems are operated in the MF to VHF bands [16]. Efficient operation at such high frequencies is not possible at high power due to limitations with current semiconductor devices.

The Power Pads of Fig. 4 overcome several limitations of common couplers by using multiple smaller bars held in place by a shock absorbing coil former with further protection provided by the aluminum and plastic case. Power pads are thin compared to standard core topologies and are lighter than conventional circular coupler designs that use solid ferrite discs. A 2kW pad system capable of operating with an air gap of approximately 200mm was presented in [7]. Here the length of the ferrite bars was the most important factor relating to the ability of this structure to achieve the necessary separations desired (in this case the pad was optimized for 200mm separation). This resulted in a 700mm diameter pad constructed with twelve ferrite spokes made up of three standard ferrite 'I' bars (93mmLx28mmWx16mmT). The coil consists of 25 turns of 4mm diameter Litz wire. The measured and simulated performance at 20kHz with a current of 23A is shown in Fig. 5. With the P_{su} shown it can deliver 2kW with $Q < 5$ within ± 100 mm, but for larger tolerances a much larger pad would be required.

While such structures are ideally suited to stationary charging, a power null occurs when the secondary is offset from the primary by approximately 40% of the pad diameter.

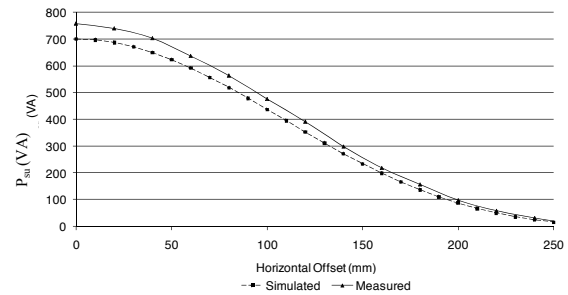


Figure 5: Simulated and measured horizontal profiles at 210mm separation with a primary current of 23ARMS at 20kHz

Furthermore flux is launched from the centre of the transmitter pad to return at the outer edge of the pad so that the field lines only extend upwards to a useful height of approximately $\frac{1}{4}$ of the pad diameter. For roadway applications, significantly larger pads would be required. Finally, if circular pads were placed side by side along a highway as indicated by Fig. 2 there would also be unavoidable nulls in power transfer between pads, so that each pad would have to transfer peaks of twice the average power demand to ensure adequate power transfer. These fundamental limitations mean that circular pads are not suited for a dynamic roadway system.

To overcome the shortcomings of the circular pad structure, a new battery charging magnetic structure using bars has been proposed [17-19]. This bar pad structure creates essentially a horizontal flux profile compared with the vertical fields of the circular pads as shown in the comparisons of Fig. 6(a) and (b). The advantage of this structure is that the field naturally achieves a higher height and therefore the coupled power to a receiver designed to capture the horizontal (rather than vertical) field is improved.

The coupling factor, κ , shown by (2), provides a useful measure for comparing the magnetic properties of different pad topologies. The track and receiver pads of these charging structures are typically constructed to have an almost identical magnetic structure. For the purpose of evaluation each pad can be made to have the same number of turns, although in practice the turns will be chosen based on output current and voltage demands. Improved coupling significantly increases the system efficiency and power transfer at a given current and frequency as indicated by (1).

$$\kappa = \frac{N_2 M}{N_1 L_2} \quad (2)$$

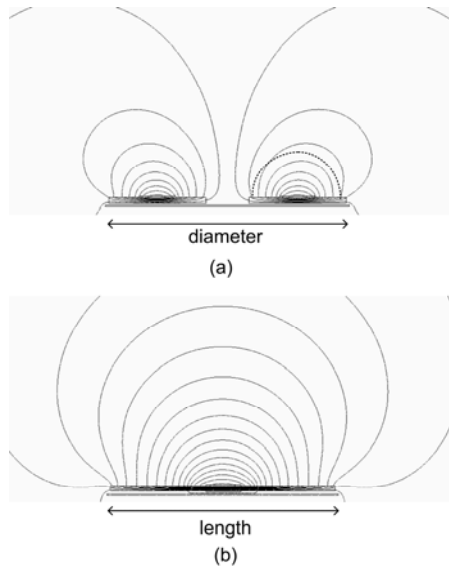


Figure 6: 2D flux plots for (a) circular (b) bar track pads

As shown in [17, 18] the design of the flat pad is significantly improved if a flux pipe is introduced as shown in Fig. 7 with coils placed at either end to drive the flux from one pole through the ferrite bar structure to the other pole end. The pole ends are then designed to efficiently launch and capture the flux to achieve good coupling.

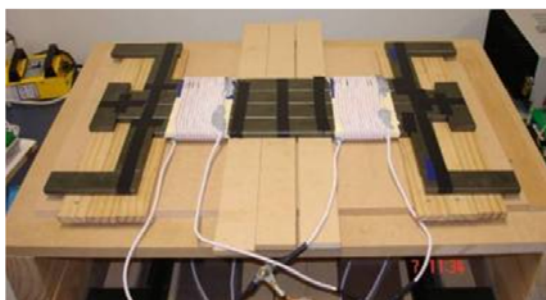
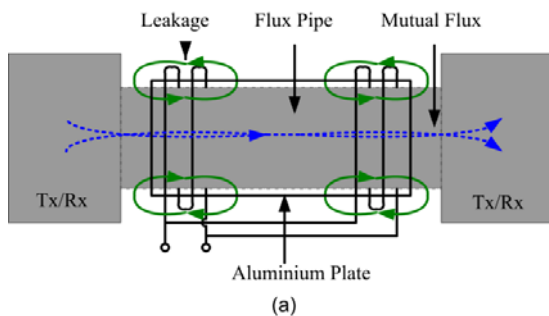


Figure 7: A horizontal flux pad with flux pipe (a) concept with coils in parallel (b) prototype flux pipe with two 15 turn coils

A comparison of this new “flux pipe” pad against a 700mm diameter circular pad is shown in Table 1 and Fig. 8, with both pads excited at 20 kHz and

23A. This new pad uses essentially the same number of ferrites, but only 42% of the wire and therefore copper losses are significantly reduced. This “flux pipe” pad structure of Fig. 7 is polarized, unlike the circular pads described earlier, and therefore comparisons need to be made in terms of offsets in all x , y , and z axes. Despite the area of the pad being significantly smaller, the results show a clear improvement in coupling factor for vertical (z) separations above 120mm (Fig. 8(a)) and at the desired 200mm separation point, significantly better coupling for all lateral offsets in the x or y directions (Fig. 8(b)). The uncompensated power (P_{su}) at 200mm separation (from Table 1 below) is clearly superior, clearly indicating that the flux pipe is a lighter and more cost effective design. Furthermore this flux pipe design allows 2kW to be transferred within a ~200mm radius of the pad centre, which is a significant improvement. The ferrite is utilized far more effectively in the flux pipe and the power transfer density is significantly higher allowing compact pads that simplify mounting on EVs. The power drops off slowly in the y axis (along the direction of the highway), so that if these pads are placed along a highway and configured such that they are driven synchronized, in phase, then it is possible to deliver a power profile that is always available to a vehicle without the power nulls that would arise from cascaded circular pads. Power transfers of 10kW can be achieved by increasing the pad current and operating frequency, but achieving this with a very large horizontal (x) tolerance is still demanding. An alternative approach with significantly improved horizontal tolerance using a multiphase pad is described following.

TABLE 1: Circular v.s. Flux Pipe

Parameter	Circular v.s. Flux Pipe		Units
	Circular pad	Flux Pipe	
Number of Ferrites	36	34	
Length of Wire	31	13	m
Area	0.38	0.22	m ²
Coupling @200mm.	0.16	0.2	M/L_2
P_{su} @ 200mm	775	1211	VA
$P_{su}/Area$ @ 200mm.	2039	5505	VA/m ²
$P_{su}/Vol.Fe$ @200mm	0.51	0.85	VA/cm ³

3.2 Multiphase Charging Pads

In order to improve horizontal tolerance, a bipolar three phase track topology was proposed in [20]. This track uses overlapping phase wires driven from a three-phase inverter. The overlapping nature of the track phases results in currents that

differ by 60° in each adjacent wire in a similar manner to windings in a cage induction motor. This creates a travelling field across the width of the track which results in a wide and even power profile that a simple receiver pad can capture. Such a simple receiver captures horizontal flux similar to the flux pipe discussed in the previous section. However, a consequence of having overlapping tracks is the presence of mutual inductance between phases. This means that energy from one track phase can couple into adjacent phases, similar to the power coupling between each track conductor and the receiver. Overcoming this problem is possible but expensive.

Alternatively, a unipolar three phase track topology structured as in Fig. 9 can be used (named because there are no explicit return conductors). Notably the horizontal tolerance of the receiver is now determined by the width of the track rather than simply its resonant current rating. Increasing tolerance requires making the track wider and this added length increases the copper loss linearly.

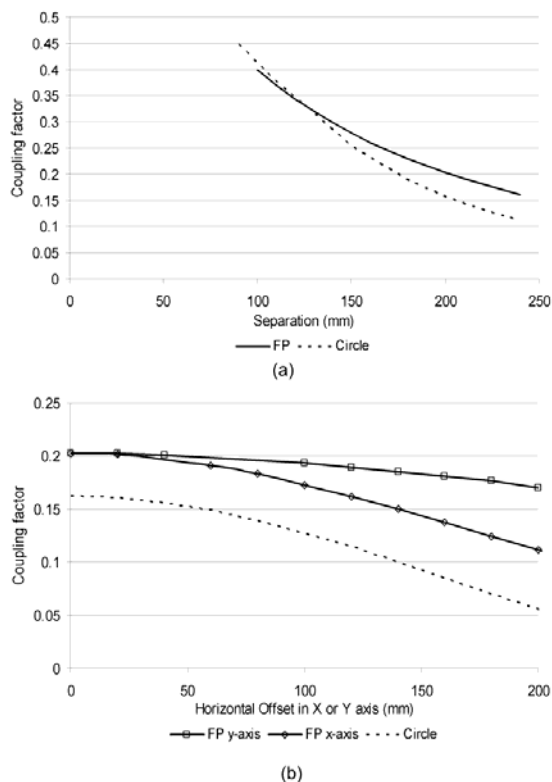


Figure 8: Profiles of circular and flux pipe (FP) pads (a) with vertical separation (z) and (b) horizontal (x and y) offsets at 200mm separation

A range of parameters affect the output power of such a system, including: the magnetic length, width, and thickness of the receiver pad, the track pitch and width, and the design of the ferrite structure under the track. These were investigated by simulation and reported [21], resulting in a prototype design for a pad for the DIPT system. The pad operates with an air gap of $z = 175\text{mm}$. In this evaluation the receiver is simplified to that of a simple bar with a single winding to aid analysis. Results show that if it is made to be four times the pitch of the track with a winding that covers around 80% of the receiver ferrite almost all of the available horizontal flux is captured [21]. The total track width evaluated was 1550mm, corresponding to a midsection width of 800mm and a pitch of 250mm. The receiver was therefore 1m long and had a width of 0.3m. Ferrite is also required underneath the track to enhance coupling. Various options were considered from a full ferrite sheet to ferrite strips. Eight 20mm wide ferrite strips with a relative permeability of 2000 placed equidistantly under the straight section of the track were found to give good performance.

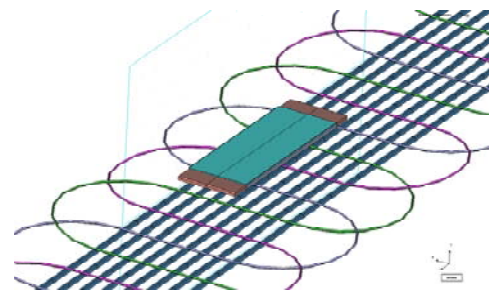


Figure 9: A prototype three phase unipolar wave wound transmitter pad, with simple horizontal bar receiver.

The resulting power profile is shown in Fig. 10. Here the track current/phase was set to 250A which is typical for industrial IPT systems. The chosen frequency was also increased to $\sim 40\text{kHz}$. Each line represents the available P_{su} with the receiver positioned at $z=175\text{mm}$ separation but at various offsets from the centre and moving in the y direction (along the track) over a length equal to a full 360° movement. Here $x=0\text{mm}$ represents operation along the track centre, while an $x=400\text{mm}$ offset represents operation while moving close to the edge of the track where the wires loop back. As expected power falls off dramatically at this point, as flux essentially cancels. The small ripple shown results from the curved end sections. Assuming a Q of 5 is

allowable a constant 30kW can be coupled over an 800mm wide zone to an EV if desired.

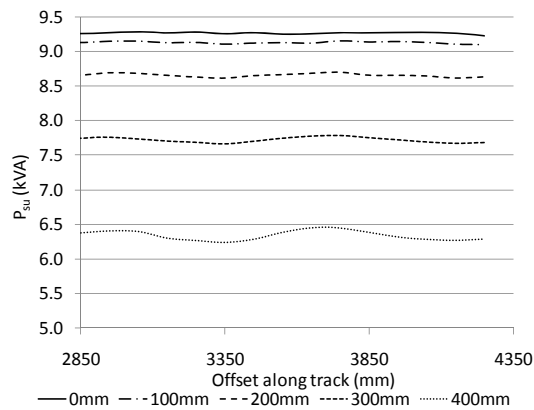


Figure 10: Performance of a three phase unipolar transmitter pad with receiver at 175mm vertical separation.

3.3 A Possible Stationary and Dynamic System

From the above results it seems feasible that a DIPT system could be created for EVs. The vehicle would be fitted with one or more relatively simple receiver pads (such as the flux pipe receiver described earlier) placed underneath. Such a pad can couple power and receive charge when the EV is parked stationary over a similar “flux pipe” power pad on the ground, but can also couple power dynamically from a roadway system constructed of either single or multiphase power pad structures as described above.

As shown in [2] these systems have both horizontal and vertical components of flux in both single and multiphase systems, so that these systems can benefit if a quadrature (essentially two phase) power receiver is used, rather than the simple horizontal flux receiver described for the flux pipe or bar shaped receivers. This only requires a second coil configured to capture the vertical flux and suitable processing electronics.

4 Charging using Dynamic Demand Control

4.1 Dynamic Demand Control Concepts

To evaluate the advantages that DDC could bring, an IPT battery charging system operating from single phase mains with DDC was developed for evaluation purposes. The system is shown conceptually in Fig. 11. The power supply presented in [22] was used here. It outputs a

regulated current at a fixed frequency of 20 kHz into the ground pad of the battery charger system. This power supply has minimal DC energy storage, good input mains power factor and efficiency. A feature of the power supply is that the DC link in the power supply, and hence the track current I_1 , is amplitude modulated at twice the mains frequency due to the minimal DC energy storage. For DDC the pick-up controller topology needs to be able to regulate its output power on a continuous basis or in multiple small steps like those discussed in [23, 24]. An LC parallel tuned AC-AC pick-up controller presented in [23] is used simply because it has high efficiency and fast response, and the capability to vary the output power continuously from no load to full load. The primary and secondary charging pads used in this system are the circular lumped coil types as discussed in section 3.1 and presented in [25, 7].

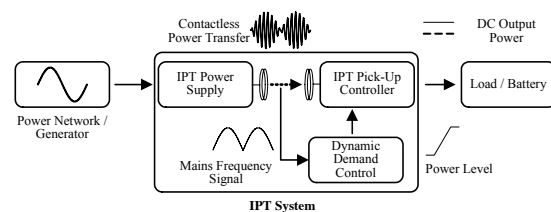


Figure 11: Overview of an IPT charging system with DDC.

The role of the dynamic demand controller is to send the desired output power level to the pick-up controller based on the measured grid frequency. The frequency window used in this system is set but not limited to 49.5–50.5 Hz. In this range, the battery charging system should operate linearly from no load to full power as shown in Fig. 12.

As the primary track current envelope is amplitude modulated at the grid frequency, the induced voltage in the secondary is also modulated enabling the grid frequency to be simply measured on the secondary (vehicle) side without complicated circuitry. For systems with constant track current envelopes, an alternative method would be needed.

3.2 An Evaluation System

A simple block diagram of the global control system is shown in Fig. 11. It comprises a power network/generator (without any governor action) and a battery charging system.

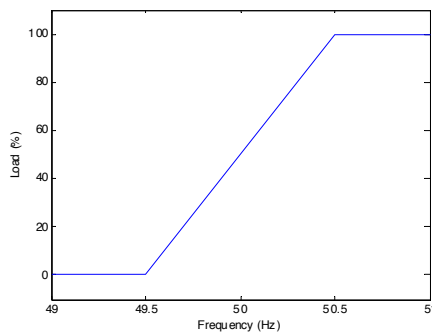


Figure 12: Output power and frequency characteristic with DDC.

In the block diagram, the power network is simply modeled as a rotational body with inertia J (Nm^2), and “ k ” is a droop factor ($\text{Nm}/(\text{rad}/\text{sec})$), which is essentially the slope of the line in Fig. 12. For the example shown, the line rises from zero to rated torque in 1Hz or 2% of rated speed. For a 2-pole generator rated at 7.5 kW used here for the laboratory measurements, “ k ” would be 25 $\text{Nm}/6.28$ radians/sec or approximately 4 $\text{Nm}/(\text{rad}/\text{sec})$. T is the frequency measurement time constant and as shown is assumed to be that of a first order system. Without the battery charging system, any torque variation ($\Delta\tau$) applied to the generator results in a system frequency deviation ($\Delta\omega$) (assuming a constant consumer loading condition). Using the dynamic demand control IPT system, $\Delta\tau$ is then reduced from the power network/generator by varying the power delivered to the load/battery according to $\Delta\omega$. This results in an appropriate change to the grid frequency keeping it within the preset window.

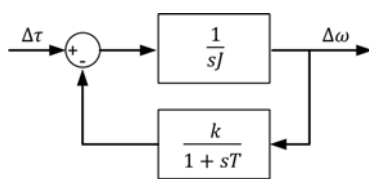


Figure 13: Block diagram of the control system.

Using the usual symbols for torque speed etc. the transfer function for the change in speed to a change in torque is given by:

$$\frac{\Delta\omega}{\Delta\tau} = \frac{1+sT}{JT s^2 + Js + k} \quad (3)$$

For this system the damping factor, settling time, and steady state error are given by:

$$\zeta = \frac{1}{2} \sqrt{\frac{J}{Tk}}, t_s \approx \pi \sqrt{\frac{JT}{k}}, \Delta\omega = \frac{\Delta\tau}{k}$$

Thus for the 2-pole generator as above, assuming a small system inertia of 0.35 kGm^2 and a 100 ms

filter time constant, the damping factor is 0.47, the settling time is approximately 0.3 s and the speed offset is 0.25 radian/sec per Nm. This example considers but a tiny system – corresponding to the experimental example following. Larger systems would have much higher inertias giving better damping factors but the same offset dependent on the slope of the line in Fig. 12. To get faster response the measurement time constant may be reduced but this leads to a significantly worse damping factor.

To measure the performance of the frequency measurement technique, the proposed battery charging system was driven from a single phase variable frequency AC supply (Agilent AC power source 6813B) with the system operating under full power conditions. The frequency was varied slowly from 49.5 Hz to 50.5 Hz. Partial measured results are presented in Fig. 14 (upper trace) where it is apparent that individual measurements are significantly affected by noise. To improve this, the measured results were filtered using a rolling average of eight measurements after which a frequency variation of 0.01 Hz is now discernible as shown in Fig. 14 (lower Trace).

For evaluating the performance of the dynamic demand control IPT system, a programmable standalone power generation system was constructed comprising a variable speed drive (VSD), a 3 phase induction motor and a 3 phase AC generator. This system was set up to generate 230 V 50 Hz (per phase) and is capable of delivering up to 7 kW total. The IPT charging system was connected to one phase, while constant resistive loads were connected to the remaining two phases to emulate a constant consumer load demand. To emulate a power network with high penetration of time-variable renewable energy sources (e.g. wind energy), the VSD was configured to operate the induction motor in a torque-controlled state where the desired speed was set to the maximum value but the actual speed is limited by the torque demand. Changes to the torque-demand cause the generator to accelerate or decelerate. A random but repeatable pattern of torque commands with a distribution close to a Weibull pdf was used as the torque input to the VSD as shown in the top trace of Fig. 15. In this way a highly variable isolated power system with statistical properties close to that of a wind was created with the ideal feature that the numerical sequence could be repeated to make different measurements on the same data.

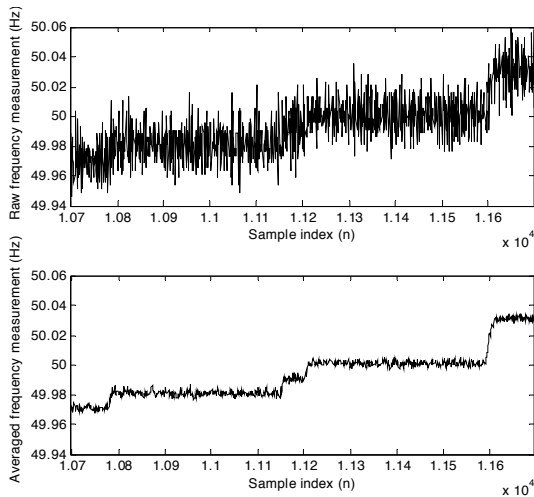


Figure 14: Raw frequency measurements (top) and averaged frequency measurements (bottom)

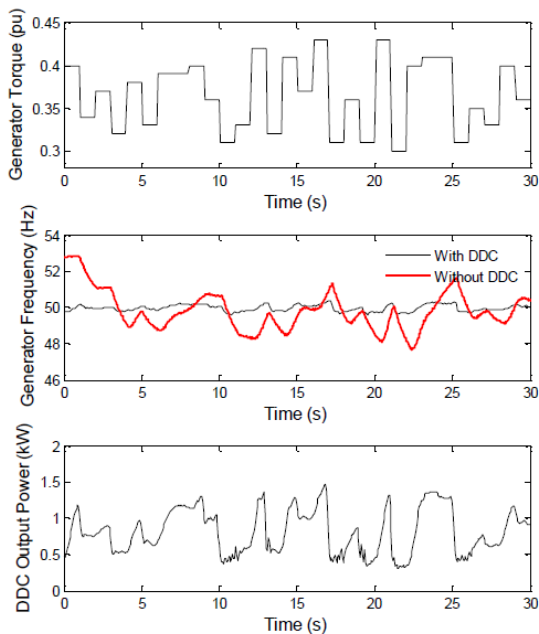


Figure 15: Measured generator frequency and charging system output power (middle and bottom) when the motor-generator set is driven with a random torque pattern (top)

The system was operated in a steady-state mode and a sequence of 50 random torques was input to the VSD at one second intervals to emulate a changing wind pattern. With the dynamic demand IPT battery charging system connected to the generator, the system frequency of the generator and the output power of the charging system were then measured under battery charging conditions. Using an identical torque sequence the system frequency was also measured with the battery charger behaving like a static load (without DDC). The measured results from the 30 second

samples for both experiments are shown in Fig. 15 (middle trace) while the measured frequency distributions are presented in Fig. 16.

Without DDC in place, the measured generator frequency is unstable and varies from 47 Hz to 53 Hz. By any measure this is a power supply of very low quality and has limited usefulness. By comparison, with DDC employed (as shown on the same traces of Fig. 15 and 16 for comparison), the frequency of the generator is successfully maintained within the preset window of 49.5 to 50.5 Hz. A comparison of the torque pattern input to the generator and the output power profile of the charging system of Fig. 15 (bottom trace) clearly shows how closely the output power profile follows the input torque pattern. As the torque limit of the induction motor is increased, the frequency speeds up but the charging system absorbs this excess power and removes the excess torque from the generator to roughly maintain the system frequency. Conversely, as the torque limit is decreased, the generator slows down forcing the charging system to reduce its power consumption, thereby reducing the total frequency change.

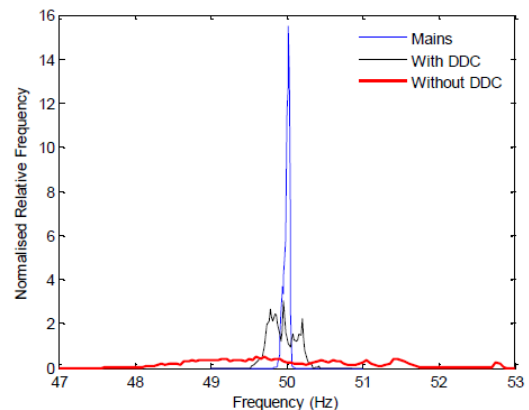


Figure 16: Generator frequency distribution with and without DDC

The measured results of the dynamic demand control experiment with an emulated fluctuating power network clearly demonstrate how a DDC controlled IPT battery charger can offer considerable frequency smoothing by adjusting its output power according to deviations in the supply frequency. A large scale deployment of battery EV's having chargers that operate under DDC could act as a controlled distributed load that automatically improves the stability of any supply network, without the need for complicated high bandwidth centralized communication infrastructures. This reduces the required

governor activity of spinning reserve and increases the wind power penetration without significant increase of grid demand-supply balancing cost. However, care needs to be taken to consider the regional supply-and-demand balance to prevent an unwanted increase of Tie-line flow as discussed in [26]. In principle this approach can also be used on very large roadway systems as the vehicles move.

5 Conclusions

As shown in this paper, it is now technically feasible to supply power to moving EV's such that the on-board battery can be significantly reduced. The system introduced here is fully modular and widely applicable, and allows the grid to extend to the roadway which provides the lowest cost EV's of all possible architectures. Wind or other green power can be wheeled through the grid to allow the dynamic battery load to match generation to demand in the rest of the network.

References

- [1] A. Brooker, M. Thornton and J. Rugh. *Technology Improvement pathways to cost effective vehicle electrification*, SAE 2010 World Congress, Detroit, Michigan April 13-15 2010.
- [2] G.A.J. Elliott, S. Raabe, G.A. Covic and J.T. Boys. *Multi-phase pick-ups for large lateral tolerance contactless power transfer systems*, IEEE Trans. Industrial Electronics Society, 57, no 5, pp 1590-1598, May 2010.
- [3] E. Valsera-Naranjo, A. Sumper, P. Lloret-Gallego, R. Villafafila-Robles and A. Sudria-Andreu. *Electrical vehicles: State of art and issues for their connection to the network*, Electrical Power Quality and Utilisation, 2009. EPQU 2009. 10th International Conference on, 2009, pp. 1-3.
- [4] C. Liuchen. *Recent developments of electric vehicles and their propulsion systems*, Aerospace and Electronic Systems Magazine, IEEE, vol. 8, no. 12, pp. 3-6, 1993.
- [5] Z. Pantic, B. Sanzhong and S. M. Lukic. *Inductively coupled power transfer for continuously powered electric vehicles*, Vehicle Power and Propulsion Conference, 2009. VPPC '09. IEEE, 2009, pp. 1271-1278.
- [6] J.G. Bolger, F.A. Kirsten and L.S. Ng. *Inductive power coupling for an electric highway system*, IEEE 28th Vehicular Technology Conference, 1978, pp. 137-144.
- [7] M. Budhia., G.A. Covic and J.T. Boys. *Design and Optimisation of Magnetic Structures for Lumped Inductive Power Transfer Systems*, The inaugural IEEE Energy Conversion Conference and Exposition, ECCE 2009, San Jose California, United States, Sept. 20-24., 2009, pp. 2081-2088
- [8] S. Valtchev, B. Borges, K. Brandisky and J. B. Klaassens, *Resonant Contactless Energy Transfer With Improved Efficiency*, IEEE Transactions on Power Electronics, vol. 24, no. 3, pp. 685-699, 2009
- [9] D.A.G. Pedder, A.D. Brown and J.A. Skinner. *A contactless electrical energy transmission system*, IEEE Transactions on Industrial Electronics, vol. 46, no. 1, pp. 23-30, 1999.
- [10] F. Nakao, Y. Matsuo, M. Kitaoka and H. Sakamoto. *Ferrite core couplers for inductive chargers*, Proceedings of the Power Conversion Conference, 2002. PCC Osaka 2002, pp. 850-854 vol.2.
- [11] H. Sakamoto, K. Harada, S. Washimiya, K. Takehara, Y. Matsuo and F. Nakao. *Large air-gap coupler for inductive charger [for electric vehicles]*, IEEE Transactions on Magnetics, vol. 35, no. 5, pp. 3526-3528, 1999.
- [12] K. Chang-Gyun, S. Dong-Hyun, Y. Jung-Sik, P. Jong-Hu and B. H. Cho. *Design of a contactless battery charger for cellular phone*, IEEE Transactions on Industrial Electronics, vol. 48, no. 6, pp. 1238-1247, 2001.
- [13] S.Y.R. Hui and W.W.C. Ho. *A new generation of universal contactless Battery Charging platform for portable Consumer Electronic equipment*, IEEE Transactions on Power Electronics, vol. 20, no. 3, pp. 620-627, 2005.
- [14] L. Xun and S.Y. Hui. *Simulation Study and Experimental Verification of a Universal Contactless Battery Charging Platform With Localized Charging Features*, IEEE Transactions on Power Electronics, vol. 22, no. 6, pp. 2202-2210, 2007.
- [15] J. L. Villa, J. Sallán, A. Llombart and J. F. Sanz. *Design of a high frequency Inductively Coupled Power Transfer system for electric vehicle battery charge*, Applied Energy, vol. 86, no. 3, pp. 355-363, 2009.
- [16] L. Xun, W. M. Ng, C. K. Lee and S. Y. Hui. *Optimal operation of contactless transformers with resonance in secondary circuits*, 23rd Annual IEEE Applied Power Electronics Conference and Exposition, 2008. APEC 2008.,

2008, pp. 645-650.

- [17] J.T. Boys, C.-Y. Huang. *Inductive Power Transfer Apparatus* WO2010/090538, patent pending, 5-02-2009
- [18] M. Budhia, G.A. Covic, and J.T. Boys. *A New Magnetic Coupler for Inductive Power Transfer Electric Vehicle Charging Systems* 36th Annual Conference of the IEEE Industrial Electronics Society, IECON 2010, Phoenix AZ, USA, Nov. 7-10, 2010, pp. 2482-2492
- [19] Y. Nagatsuka, N. Ehara, Y. Kaneko, S. Abe and T. Yasuda. *Compact contactless power transfer system for electric vehicles*, International Power Electronics Conference (IPEC), 2010, pp. 807-813.
- [20] G.A. Covic, J.T. Boys, M.L.G. Kissin and H.G. Lu. *A Three-Phase Inductive Power Transfer System for Roadway-Powered Vehicles*, IEEE Transactions on Industrial Electronics, vol. 54, no. 6, pp. 3370-3378, 2007.
- [21] M. Budhia, G.A. Covic and J.T. Boys. *Magnetic Design of a Three-Phase Inductive Power Transfer System for Roadway Powered Electric Vehicles*, IEEE Vehicle power and propulsion conference, VPPC'10, Lille, France, Sept. 1-3, 2010.
- [22] J.T. Boys, C.-Y. Huang and G.A. Covic. *Single-phase unity power-factor inductive power transfer system*, IEEE, Power Electronics Specialists Conference, 2008. PESC 2008. 2008, pp. 3701-3706.
- [23] H.H. Wu, J.T. Boys and G.A. Covic. *An AC Processing Pickup for IPT Systems*, IEEE Transactions on Power Electronics, vol. 25, no. 5, pp. 1275-1284, May, 2010
- [24] C.-Y. Huang, J.T. Boys, G.A. Covic and M. Budhia. *Practical considerations for designing IPT system for EV battery charging*, IEEE Vehicle Power and Propulsion Conference, 2009. VPPC '09, 2009, pp. 402-407.
- [25] Y. Kamiya, M. Nakaoka, T. Sato, J. Kusaka, Y. Daisho, S. Takahashi and K. Narusawa. *Development and performance evaluation of advanced electric micro bus equipped with non-contact inductive rapid-charging system*, 23rd International Electric Vehicle Symposium, Anaheim, USA, 2007, pp. 1-14.
- [26] M. Takagi, K. Yakaji, H. Yamamoto. *Power System Stabilization by charging power management of Plug-in Hybrid Electric Vehicles with LFC signal*, IEEE Vehicle Power and

Propulsion Conference, 2009, VPPC '09, 2009, pp. 822-826

Authors



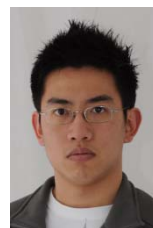
Associate Prof. Grant Covic heads power electronics research at the University of Auckland (UoA). His current research and consulting interests include power electronics, electric vehicle battery charging and inductive (contact-less) power transfer (IPT). Was co-founder and head of research of "HaloIPT" until sale.



John T. Boys is Professor of Electronics at the UoA. His specialist research areas are power electronics and inductive power transfer. He is a Fellow of the Royal Society of New Zealand and a Distinguished Fellow of the Institution of Professional Engineers New Zealand.



Mickel Budhia received the B.E. degree in Electrical and Electronic Engineering from The UoA, in 2008 and recently submitted his Ph.D. degree at the UoA. His research interests include analyzing and designing magnetic components for inductive power transfer systems for EV charging.



Chang-Yu Huang received his BE Hons, ME Hons, and PhD from The UoA, New Zealand in 2004, 2006, 2012 respectively. He is currently a postdoctoral candidate at The UoA. His fields of interest include EV charging, resonant converters and inductive power transfer.